IEEE Access
Multidisciplinary | Rapid Review | Open Access Journal

Received September 20, 2019, accepted October 14, 2019, date of publication October 22, 2019, date of current version October 31, 2019.

Digital Object Identifier 10.1109/ACCESS.2019.2948864

Cooperative Positioning for Multi-AUVs Based on Factor Graph and Maximum Correntropy

SHIWEI FAN[1], YA ZHANG[1], QIANG HAO[1], PAN JIANG[1], CHUNYANG YU[2], AND FEI YU[1]
[1]School of Instrumentation Science and Engineering, Harbin Institute of Technology, Harbin 150001, China
[2]Department of Geomatics Engineering, University of Calgary, Calgary, AB T2N 1N4, Canada

Corresponding author: Ya Zhang (yazhang@ hit.edu.cn)

This work was supported in part by the National Natural Science Foundation of China under Grant 51709068, and in part by the Postdoctoral Foundation of Heilongjiang Province Government under Grant LBH-Z17094.

ABSTRACT Cooperative positioning (CP) is considered as a promising positioning method for multiple autonomous underwater vehicles (multi-AUVs), because CP is characterized by low cost and high precision. In this research, a novel autonomous underwater vehicle (AUV) CP algorithm is proposed to enhance the global localization accuracy of the follower AUV. However, in traditional CP algorithm, the positioning error is large under the condition that the outlier data exists in the observation, which happens commonly. So in this research, a novel CP algorithm based on the factor graph and maximum correntropy(FGMC) for AUV is proposed to enhance the global localization accuracy of the AUV. Different from the traditional algorithms, this presented FGMC-based CP algorithm implements mathematically the Bayes filter by converting the global function estimation problem into the local one. And furthermore, the maximum correntropy is used as the cost function in the factor graph to estimation problem, this can reduce the influence of outliers on positioning accuracy. FGMC based cooperative positioning algorithm is established to mathematically implement the Bayes filter by converting the global function estimation problem into local function estimation problem. Furthermore, the maximum correntropy is used as the cost function in the factor graph to estimate the variables. To demonstrate and verify the proposed algorithm, simulation and real tests in different scenarios are performed in this research. Compared with the traditional CP algorithms, the positioning error of the proposed FGMC cooperative positioning algorithm is obviously smaller than that of the other algorithms.

INDEX TERMS Cooperative positioning, AUV, factor graph, maximum correntropy.

I. INTRODUCTION

The primary issue in ensuring the successful and efficient execution of autonomous underwater vehicles (AUVs) and other marine robots is accurate positioning [1]–[3]. Common methods based on inertial measurement units (IMUs) have irreplaceable merit with respect to independencies, however, the accumulated error prevents high-accuracy localization in large-scale environments. Compared with using advanced IMUs, incorporating external information is a more feasible solution. In most terrestrial environments, the Global Navigation Satellite System (GNSS) or Wi-Fi can be used to locate an autonomous vehicle [4]–[7]. However, for AUV, GNSS cannot be used due to the strong attenuation of electromagnetic fields under water [8]. In the harsh underwater environment, high-precision navigation has become an urgent and arduous challenge for AUV [9], [10].

The associate editor coordinating the review of this manuscript and approving it for publication was Xiangxue Li.

Without an external reference, such as GNSS, the vehicle must rely on proprioceptive information obtained through a compass, a Doppler Velocity Logger (DVL) or an Inertial Navigation System (INS) [11]–[13].

The advantage of using compass and DVL for positioning is low cost, and Dead-Reckoning(DR) method is usually used for positioning in this case. But the positioning error based on DR information grows without bound. In the range of a few hundred meters from the sea floor, the positioning error is generally 0.5%− 2% of the mileage, so the DVL will be locked when working under the sea [14]. Errors as low as 0.1% can be obtained with large and expensive INS systems, however, the cost will be enormous if each AUV is equipped with high-precision INS. AUV can avoid error accumulation by surfacing to receive GPS signals, but this is impossible for many applications such as deep sea navigation [15].

Generally, the cost and the accuracy are the key issues we need to consider about for AUV navigation system [16], [17]. To reduce costs, usually only the leader AUV is equipped

with high precision INS systems, and the rest of the follower AUV are equipped with compasses and DVLs to calculate the position. Underwater acoustic devices are commonly used for acoustic communication and distance measurement between AUVs. And follower AUV fuse data from underwater acoustic devices to improve the position accuracy. However, due to the complicated working environment and the limitation of sensor performance parameters, cooperative positioning system (CPS) has the problem of inaccurate statistical characteristics of system noise, affecting state estimation performance. In addition, subjected to the influence of complex underwater acoustic communication environment, the underwater acoustic distance measurement information is often interfered by abnormal measurement noise, whose distribution often exhibits heavy tail distribution characteristics. Therefore, the main challenge for AUVs is to design an efficient structure and algorithm to fuse information with outliers from multiple AUVs.

As a classical nonlinear filtering algorithm, Extended Kalman Filter (EKF) is widely used in recursive estimation of AUV positions. In [18], the performance of particle filter (PF), non-linear least-squares optimization (NLS) solution and EKF is compared. Although the post-processed NLS solution achieves the best performance, it is not available online for AUV. For PF, it is considered less suitable for cooperative positioning of AUVs since that large particle clusters are needed to adequately sample large uncertainty areas. Since that EKF is based on the principle of linearized nonlinear system model by utilizing first-order Taylor series, so it is easy to operate and fast to implement, and is widely used in the cooperative positioning of underwater vehicles. However, the estimation error will be large or even divergence when the system is serious nonlinearity or the observation has outliers [19].

The unscented Kalman filter (UKF) [20] and divided difference filter (DDF) [21], [22], known as sigma-point Kalman filter (SPKF), are efficient derivative-free state estimation methods, which propagate a cluster of points centered on the current estimate to obtain improved approximations of the conditional mean and covariance rather than linearizing the dynamic system. Compared with the basic Kalman filter, UKF can easily increases the estimation accuracy when system and measurement equations are nonlinear. The performance of the UKF and DDF is nearly the same [23]. However, the error is large when there are outliers in the observed value.

So it is necessary to develop filtering approaches for cooperative positioning that are robust to measurements whose noise deviations from the assumed Gaussian distribution. One approach is the adaptive filter(e.g. Adaptive Robust Extended Kalman Filter, AREKF), which adopts an adaptive scheme to automatically tune the error covariance matrix in response to the changing environment [24]. But the variation of covariance may deteriorate the performance, and moreover, the computational complexity of this approach is large. Huber filter is also an approach to solve this problem, which is a combination of minimum l_1 and l_2 norm estimator [25]. However, the influence function of Huber's robust methodology does not decrease, which may affect the performance.

The observation noise is assumed to be Gaussian noise in [26]. And in this case, a cooperative positioning algorithm base on IFGS(IFGS algorithm for short) performs well. However, there are often special cases in underwater which lead to outliers in observation, increasing the positioning error. So it is very important to propose a method suitable for this situation.

In order to improve the positioning accuracy, a cooperative positioning algorithm base on factor graph and maximum correntropy(FGMC algorithm for short) is proposed to calculate the position information of the system when the measurement has outliers. The factor graph divides global functions into local functions, which can effectively reduce the system's computation complexity and nonlinear errors. Maximum correntropy can capture the high-order statistics of data, rather than the second-order statistics commonly used. In addition, the cost function based on maximum correlation entropy can effectively reduce the impact of outliers on system accuracy.

This paper is organized as follows. In Section 2, we introduce the mathematical model of the CPS, factor graph and maximum correntropy. Next, the FGMC algorithm is proposed in Section 3. Simulation and real test results, that compared the positioning errors of 4 different algorithms, including the proposed FGMC algorithm, are given in Section 4 and Section 5.

II. MATHEMATICAL MODELS AND THEORETICAL BASIS

A. COOPERATIVE POSITIONING SYSTEM MODEL

For multi-AUV systems, low precision navigation equipments are often equipped for autonomous navigation due to cost, energy consumption and volume, constrains the accuracy of the entire navigation system. Taking a typical DR system as an example, sensor error and installation deviation lead to an increase in DR error. In order to ensure the navigation performance of the system and suppress the positioning error, an external absolute reference information is needed as auxiliary information to correct the system error. Based on this realistic goal, cooperative positioning is proposed to correct the positioning error. Multi-AUV CPS typically include one or more leader AUVs equipped with high-precision navigation equipment (or regularly surfaced to receive high-precision GPS positioning information), follower AUVs are equipped with low precision navigation equipments. Each follower AUV receives observations from leader AUV, and the leader AUVs and follower AUVs cooperates with each other. Information is processed to improve the overall positioning performance of the entire system.

In order to simplify the analysis of the CPS problem and take the generality of the application into consideration, the DR algorithm is used to autonomously navigate the low-precision AUV. The traditional DR method can provide three dimension position. Because the height can be obtained by the depthometer easily, the 3D positioning problem is usually simplified into a 2D positioning problem.

The state of AUV plane motion is (x_k, y_k), which represents the position coordinates of AUV at k time. After obtaining the initial position coordinates of the AUV, the real-time position coordinates can be updated according to the velocity and course information measured by the sensors:

$$\begin{cases} x_k = x_{k-1} + \hat{v}_k \cos\hat{\theta}_k \Delta t \\ y_k = y_{k-1} + \hat{v}_k \sin\hat{\theta}_k \Delta t \end{cases} \tag{1}$$

where $\hat{v}_k$ is the velocity measurement of DVL along the bow direction of AUV; $\hat{\theta}_k$ is the course measured by the azimuth sensor such as compass; and Δt is the sampling time interval.

The discrete equation of state corresponding to Equation (1) is

$$X_k = F_{k,k-1} X_{k-1} + \Gamma(u_{k-1} + w_{k-1}) \tag{2}$$

where X_k is the state vector, $F_{k,k-1}$ is the state transition matrix, $\Gamma(u_{k-1} + w_{k-1})$ is the nonlinear term, $u_{k-1} = (v_{k-1}, \theta_{k-1})^T$ is the control input, $w_k = (w_{vk}, w_{\theta k})^T$ is the system process noise, including the velocity measurement noise and the course measurement noise, and the covariance matrix Q_k is

$$Q_k = \begin{bmatrix} \sigma_{v_k}^2 & 0 \\ 0 & \sigma_{\theta_k}^2 \end{bmatrix} \tag{3}$$

where $\sigma_{v_k}^2$ and $\sigma_{\theta_k}^2$ are the variances of v_k and θ_k.

AUV corrects the continuous accumulated positioning error through relative distance observation in cooperative positioning system. Because the relative distance information measured by underwater acoustic communication equipment is 3-D, it is necessary to further transform the 3-D space observation distance into 2-D space relative distance to simplify the algorithm. If the 3-D distance measurement information $z_{3,k}$ and the precise depth information h_k^l of leader AUV and h_k of follower AUV are known, the converted 2-D measurement distance z_k is expressed as

$$z_k = \sqrt{z_{3,k}^2 - (h_k^l - h_k)^2} \tag{4}$$

It is obvious that the relationship between the leader AUV position information $X_k^l = (x_k^l, y_k^l, z_k^l)$, the follower AUV position information $X_k = (x_k, y_k, z_k)$ and the corresponding distance observation equation at the moment k can also be represented as:

$$z_k = h(X_k) + \mu_k = \sqrt{(x_k^l - x_k)^2 + (y_k^l - y_k)^2} + \mu_k \tag{5}$$

where μ_k is the acoustic distance measurement noise, which is usually assumed to be a zero-mean Gaussian white noise sequence, following the gauss distribution $N(0, \sigma_k^2)$.

B. FACTOR GRAPH

Factor Graph is a kind of probability graph. There are many kinds of probability maps, the most common of which are Bayesian Network and Markov Random Fields. In probability graphs, it is a fundamental problem to find the edge distribution of a variable. There are many ways to solve this problem, one of which is to convert Bayesian Network and Markov Random Fields into Facor Graph. Factor graph is a representation of the factorization of function factors. Generally, it contains two kinds of nodes, variable nodes (i.e., X_1, X_2, X_3, X_4) and function nodes (i.e., $P(X_1)$, $P(X_2|X_1)$, $P(X_4|X_3)$ and $P(X_3|X_1, X_2)$). We know that a global function can be decomposed into the product of several local functions, and these local functions and corresponding variables can be reflected in the factor graph. By decomposing large-scale global functions, the factor graph obtains simple local functions, which indirectly improves the computational efficiency of solving large-scale networks [27]. For example, in the initial process, we can get the joint probability distribution of directed acyclic graphs, and this distribution can be expressed in the form of factor graphs. Fig.1 and Fig.2 show the directed acyclic graph and the corresponding factor graph. Directed acyclic graphs are finite digraphs without directed rings, as shown in Fig.1.

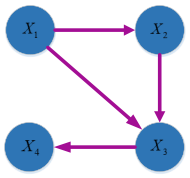

FIGURE 1. A directed acyclic graph.

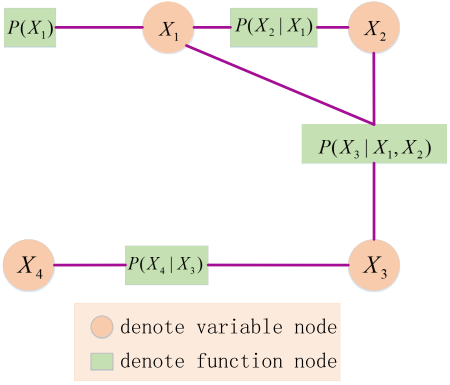

FIGURE 2. The factor graph corresponding to the directed acyclic graph in Fig.1.

According to the definition of the factor graph, we know that the factor graph is non-directional, and all neighboring nodes of one node will have the opposite type to the node itself.

C. MAXIMUM CORRENTROPY

The correntropy is a new concept to measure the generalized similarity between two random variables. Given two random variables A, B with joint distribution function $\mathbf{F}_{AB}(a, b)$, the correntropy is defined by

$$V(A, B) = E[\kappa(a, b)] = \int \kappa(a, b) d\mathbf{F}_{AB}(a, b) \tag{6}$$

where $\kappa()$ is a shift-invariant Mercer Kernel. The most popular kernel used in the correntropy is the Gaussian kernel,

and in this paper, it is given by

$$\kappa_\sigma(a,b) = \frac{1}{\sqrt{2\pi}\sigma} exp(-\frac{\| a-b \|^2}{2\sigma^2}) \tag{7}$$

where $\sigma > 0$ denotes the kernel size (or kernel bandwidth).

Compared with other similarity measures, such as root mean square error (RMSE), it has the following advantages: 1) it is bounded for any distribution; 2) it contains all even-order moments, which are useful for non-linear and non-Gaussian signal processing; 3) the weight of higher-order moments are controlled by the size of the kernel; 4) it is a measure of local similarity and has strong robustness to outliers [28]. Relevant entropy has been successfully applied in many fields, including robust regression [29], adaptive filtering [30], classification [31], and so on.

However, the joint distribution of $\mathbf{F}_{AB}$ is usually unknown in CPS, and only a limited amount of data is available. In these situations, the sample average estimator can be used to estimate the correntropy [32]:

$$V(A,B) = \frac{1}{N}\sum_{i=1}^{N} G_\sigma(e_i) \tag{8}$$

where $e_i = a_i - b_i$, a_i, b_i are samples of A and B, and $G_\sigma(\cdot)$ denotes Gaussian kernel. N is the number of sample point of the joint distribution function $\mathbf{F}_{AB}$.

Taking Taylor series expansion of the Gaussian kernel, we have

$$V(A,B) = \sum_{i=1}^{\infty} \frac{(-1)^i}{2^i\sigma^{2i}i!} E[(A-B)^{2i}] \tag{9}$$

From the above equation, we can see that the correntropy information contains the weights of all even-order moments of the error variable, and the core bandwidth σ is a parameter weighting of the second and higher order terms. The correntropy information is used to measure the similarity of two random variables in the neighborhood controlled by the kernel width σ. Once the core width σ increases, the higher-order terms will decay significantly, and the second-order terms will dominate. This property is very useful for reducing the adverse effects of outliers or impulse noise.

Given a sequence of error data e, the cost function of maximum correntropy is given by

$$J_{MC} = \frac{1}{N}\sum_{i=1}^{N} G_\sigma(e_i) \tag{10}$$

The MC based learning can be formulated as the following optimization problem [33]:

$$\hat{W} = argmax \frac{1}{N}\sum_{i=1}^{N} G_\sigma(e_i) \tag{11}$$

where $\hat{W}$ denotes the optimal solution.

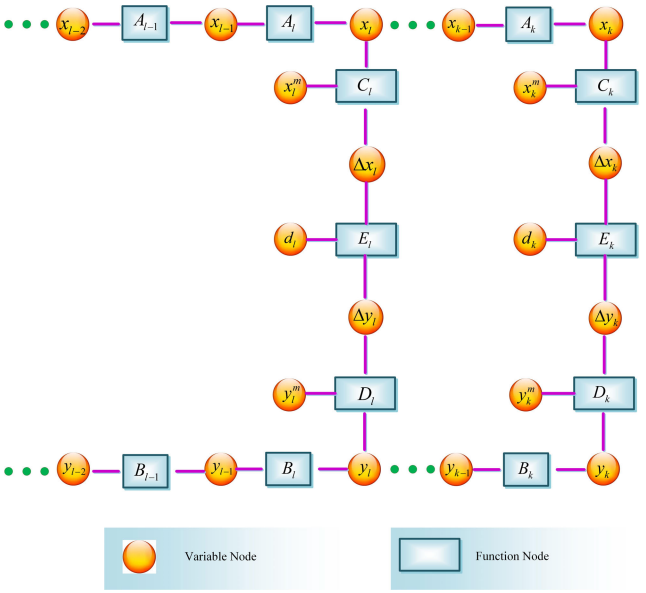

FIGURE 3. Factor graph representations of the cooperative positioning algorithm.

III. THE COOPERATIVE POSITIONING ALGORITHM BASED ON FACTOR GRAPH AND MAXIMUM CORRENTROPY

A. FACTOR GRAPH MODEL OF CPS

This paper studies the cooperative positioning method of leader-follower CPS. The AUVs are equipped with depth sensors, gyrocompass, doppler log and other sensors, as well as underwater acoustic modems that enable them to communicate acoustically with other AUVs. The leader AUV is additionally equipped with high-precision navigation and positioning equipment. The follower AUV receives the position information and distance information sent by the leader AUV. The data fusion of the follower AUV improves the positioning accuracy of the system through the cooperative positioning algorithm. In this research, the factor graph is used to convert the cooperative positioning algorithm into a graph.

The spirit of a factor graph is to convert a function with many variables into a product of functions with very few variables. In other words, the original complex function is decomposed into several simple functions, which can be solved iteratively. Distributed processing of local variables is the advantage of factor graph approach. It often provides the optimal solution or close to the optimal solution.

CP is essentially a distribution estimation problem. In the foregoing, 3-D problems of CP have been simplified into 2-D problems. Then, according to the geometric relationship between the leader AUV and the follower AUV, the 2-D estimation problem is divided into two 1-D problems. These two 1-D problems are represented by the x-coordinate group in the factor graph and the two main node groups in the y-coordinate group, respectively. And the CPS of one leader AUV is shown in Fig.3. Then, CPS with multiple leader AUVs can be similarly calculated.

The factor graph model of CPS contains 2 groups of nodes, function node and variable node, respectively. A_{l-1}, B_{l-1},A_l, B_l,C_l, D_l, E_l, A_k, B_k,C_k, D_k and E_k in the graph are function nodes. l and k represent the time. And the remaining nodes are variable nodes. x_k and y_k are the position of the follower AUV at moment k, and x_k^m and y_k^m are the position of the leader AUV at moment k. d_k is the observational distance between the leader AUV and the follower AUV at moment k. The follower AUV receives observations from leader AUV at l and k moments and fuses the data. In the absence of observations, the follower AUV carries out dead reckoning based on the position of the previous moment. Δx_k is the distance between the leader AUV and the follower AUV in the x direction. And Δy_k is the distance between the leader AUV and the follower AUV in the y direction.

B. FACTOR GRAPH SOLUTION BASED ON MAXIMUM CORRENTROPY

At the beginning of CP, it is usually easy to determine the initial position (x_0,y_0) of the follower AUV. With the initial value, the position of the follower AUV can be recursively calculated using the factor graph.

The constraints among variables in the model can be expressed by the following equations:

$$x_k = x_{k-1} + v_k \cos\theta_k \Delta t \tag{12}$$

$$y_k = y_{k-1} + v_k \sin\theta_k \Delta t \tag{13}$$

$$\Delta x_k = x_k - x_k^m \tag{14}$$

$$\Delta y_k = y_k - y_k^m \tag{15}$$

$$\Delta x_k^2 + \Delta y_k^2 = {d_k}^2 \tag{16}$$

In this research, the maximum correntropy is used as the cost function, that is, each function node represents a correntropy.

$$\begin{cases} J_{A_k} = G_\sigma\left(\|x_k - f(x_{k-1})\|\right) \\ J_{B_k} = G_\sigma\left(\|y_k - f(y_{k-1})\|\right) \\ J_{C_k} = G_\sigma\left(\left\|\Delta x_k + x_k^m - x_k\right\|\right) \\ J_{D_k} = G_\sigma\left(\left\|\Delta y_k + y_k^m - y_k\right\|\right) \\ J_{E_k} = G_\sigma\left(\left\|d_k - \sqrt{(\Delta x_k)^2 + (\Delta y_k)^2}\right\|\right) \end{cases} \tag{17}$$

where J_{A_k}, J_{B_k}, J_{C_k}, J_{D_k} and J_{E_k} are the correntropy of function nodes A_k, B_k, C_k, D_k and E_k, respectively. And $\|\bullet\|$ denotes two-norm.

If the follower AUV does not receive the observation information at $l-1$ time, then only function nodes A_{l-1} and B_{l-1} are present in the graph as in the blue box in Fig.4. The position of the follower AUV can be updated by the following formula:

$$\begin{cases} \hat{x}_{l-1} = \arg\max G_\sigma\left(\|x_{l-1} - f(x_{l-2})\|\right) \\ \hat{y}_{l-1} = \arg\max G_\sigma\left(\|y_{l-1} - f(y_{l-2})\|\right) \end{cases} \tag{18}$$

When the follower AUV receives the observation information at k time, the graph structure at this time is as shown in the black box in Fig.4. And x_k^m, y_k^m and d_k are the received information from the leader AUV. In this case, the unknown variables in the graph are x_k, y_k, Δx_k and Δy_k. x_k and y_k are the final variables to estimate. In order to estimate x_k and y_k, Δx_k and Δy_k must be obtained. The correntropy of Δx_k can be expressed as:

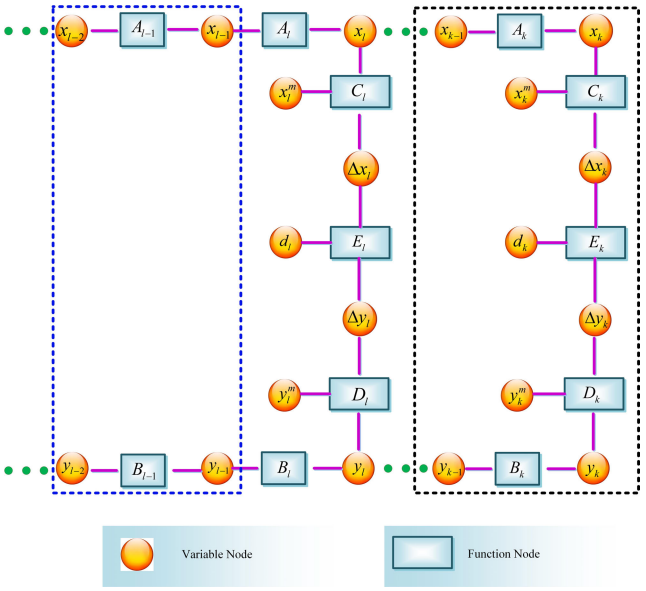

FIGURE 4. Factor graph of the CP algorithm.

$$J_{\Delta x_k} = J_{C_k} + J_{E_k} \tag{19}$$

When the correntropy of Δx_k is maximum, the estimate of Δx_k is obtained. At this point, we can obtain the following equation:

$$\begin{aligned} &\frac{\partial J_{\Delta x_k}}{\partial \Delta x_k} \\ &= \frac{\partial\left(G_\sigma\left(\left\|\Delta x_k + x_k^m - x_k\right\|\right) + G_\sigma\left(\left\|d_k - \sqrt{(\Delta x_k)^2 + (\Delta y_k)^2}\right\|\right)\right)}{\partial \Delta x_k} \\ &= \frac{\partial\left(1\Big/\left(\sqrt{2\pi}\sigma\right)\left(e^{-\frac{(\Delta x_k + x_k^m - x_k)^2}{2\sigma^2}} + e^{-\frac{\left(d_k - \sqrt{(\Delta x_k)^2 + (\Delta y_k)^2}\right)^2}{2\sigma^2}}\right)\right)}{\partial \Delta x_k} \\ &= 0 \end{aligned} \tag{20}$$

$$\begin{aligned} \Delta x_k &= x_k - x_k^m + e^{-\frac{\left(d_k - \sqrt{(\Delta x_k)^2 + (\Delta y_k)^2}\right)^2}{2\sigma^2}} \Big/ e^{-\frac{(\Delta x_k + x_k^m - x_k)^2}{2\sigma^2}} \\ &\quad \cdot \frac{\left(d_k - \sqrt{(\Delta x_k)^2 + (\Delta y_k)^2}\right)\Delta x_k}{\sqrt{(\Delta x_k)^2 + (\Delta y_k)^2}} \end{aligned} \tag{21}$$

Similarly, the correntropy of Δy_k can be expressed as:

$$J_{\Delta y_k} = J_{D_k} + J_{E_k} \tag{22}$$

When the correntropy of Δy_k is maximum, the estimate of Δy_k is obtained. At this point, we can obtain the following equation:

$$\begin{aligned}
&\frac{\partial J_{\Delta y_k}}{\partial \Delta y_k} \\
&= \frac{\partial\left(G_\sigma(\|\Delta y_k + y_k^m - y_k\|) + G_\sigma\left(\left\|d_k - \sqrt{(\Delta x_k)^2 + (\Delta y_k)^2}\right\|\right)\right)}{\partial \Delta y_k} \\
&= \frac{\partial\left(1\Big/\left(\sqrt{2\pi}\sigma\right)\left(e^{-\frac{(\Delta y_k + y_k^m - y_k)^2}{2\sigma^2}} + e^{-\frac{\left(d_k - \sqrt{(\Delta x_k)^2 + (\Delta y_k)^2}\right)^2}{2\sigma^2}}\right)\right)}{\partial \Delta y_k} \\
&= 0
\end{aligned} \tag{23}$$

$$\begin{aligned}
\Delta y_k &= y_k - y_k^m + e^{-\frac{\left(d_k - \sqrt{(\Delta x_k)^2 + (\Delta y_k)^2}\right)^2}{2\sigma^2}} \Big/ e^{-\frac{(\Delta y_k + y_k^m - y_k)^2}{2\sigma^2}} \\
&\cdot \frac{\left(d_k - \sqrt{(\Delta x_k)^2 + (\Delta y_k)^2}\right)\Delta y_k}{\sqrt{(\Delta x_k)^2 + (\Delta y_k)^2}}
\end{aligned} \tag{24}$$

x_k and y_k can only use prior estimates since x_k and y_k are not estimated when Δx_k and Δy_k are updated. Δx_k and Δy_k on the right of the equal sign of the above equation are prior estimates because no observation information is used at this time, so the following equation can be obtained:

$$\Delta x_k^- = x_k^- - x_k^m \tag{25}$$

$$\Delta y_k^- = y_k^- - y_k^m \tag{26}$$

$$\begin{aligned}
\Delta x_k &= x_k^- - x_k^m + e^{-\frac{\left(d_k - \sqrt{(\Delta x_k^-)^2 + (\Delta y_k^-)^2}\right)^2}{2\sigma^2}} \Big/ e^{-\frac{(\Delta x_k^- + x_k^m - x_k^-)^2}{2\sigma^2}} \\
&\cdot \frac{\left(d_k - \sqrt{(\Delta x_k^-)^2 + (\Delta y_k^-)^2}\right)\Delta x_k^-}{\sqrt{(\Delta x_k^-)^2 + (\Delta y_k^-)^2}} = x_k^- - x_k^m \\
&+ e^{-\frac{\left(d_k - \sqrt{(\Delta x_k^-)^2 + (\Delta y_k^-)^2}\right)^2}{2\sigma^2}} \\
&\cdot \frac{\left(d_k - \sqrt{(\Delta x_k^-)^2 + (\Delta y_k^-)^2}\right)\Delta x_k^-}{\sqrt{(\Delta x_k^-)^2 + (\Delta y_k^-)^2}}
\end{aligned} \tag{27}$$

$$\begin{aligned}
\Delta y_k &= y_k^- - y_k^m + e^{-\frac{\left(d_k - \sqrt{(\Delta x_k^-)^2 + (\Delta y_k^-)^2}\right)^2}{2\sigma^2}} \Big/ e^{-\frac{(\Delta y_k^- + y_k^m - y_k^-)^2}{2\sigma^2}} \\
&\cdot \frac{\left(d_k - \sqrt{(\Delta x_k^-)^2 + (\Delta y_k^-)^2}\right)\Delta y_k^-}{\sqrt{(\Delta x_k^-)^2 + (\Delta y_k^-)^2}} = y_k^- - y_k^m \\
&+ e^{-\frac{\left(d_k - \sqrt{(\Delta x_k^-)^2 + (\Delta y_k^-)^2}\right)^2}{2\sigma^2}} \\
&\cdot \frac{\left(d_k - \sqrt{(\Delta x_k^-)^2 + (\Delta y_k^-)^2}\right)\Delta y_k^-}{\sqrt{(\Delta x_k^-)^2 + (\Delta y_k^-)^2}}
\end{aligned} \tag{28}$$

where x_k^- and y_k^- are obtained from equation (18).

Once Δx_k and Δy_k are estimated, x_k and y_k can be solved. The correntropy of x_k can be expressed as:

$$J_{x_k} = J_{A_k} + J_{C_k} \tag{29}$$

According to the maximum correntropy criterion, we can obtain the following equation:

$$\begin{aligned}
\frac{\partial J_{x_k}}{\partial x_k} &= \frac{\partial\left(G_\sigma\left(\|x_k - f(x_{k-1})\|\right) + G_\sigma\left(\left\|\Delta x_k + x_k^m - x_k\right\|\right)\right)}{\partial x_k} \\
&= 0
\end{aligned} \tag{30}$$

$$\begin{aligned}
x_k &= x_k^- + e^{-\frac{\left(x_k^m + \Delta x_k - x_k^-\right)^2}{2\sigma^2}} \Big/ e^{-\frac{\left(x_k^- - x_k^-\right)^2}{2\sigma^2}} \left(x_k^m + \Delta x_k - x_k^-\right) \\
&= x_k^- + e^{-\frac{\left(x_k^m + \Delta x_k - x_k^-\right)^2}{2\sigma^2}} \left(x_k^m + \Delta x_k - x_k^-\right)
\end{aligned} \tag{31}$$

And the correntropy of y_k can be expressed as:

$$J_{y_k} = J_{B_k} + J_{D_k} \tag{32}$$

Similar to x_k, we can get the following equation:

$$\begin{aligned}
\frac{\partial J_{y_k}}{\partial y_k} &= \frac{\partial\left(G_\sigma\left(\|y_k - f(x_{k-1})\|\right) + G_\sigma\left(\left\|\Delta y_k + y_k^m - y_k\right\|\right)\right)}{\partial y_k} \\
&= 0
\end{aligned} \tag{33}$$

$$\begin{aligned}
y_k &= y_k^- + e^{-\frac{\left(y_k^m + \Delta y_k - y_k^-\right)^2}{2\sigma^2}} \Big/ e^{-\frac{\left(y_k^- - y_k^-\right)^2}{2\sigma^2}} \left(y_k^m + \Delta y_k - y_k^-\right) \\
&= y_k^- + e^{-\frac{\left(y_k^m + \Delta y_k - y_k^-\right)^2}{2\sigma^2}} \left(y_k^m + \Delta y_k - y_k^-\right)
\end{aligned} \tag{34}$$

In order to describe the estimation process more clearly, the pseudo code of the FGMC algorithm can be expressed in Table 1. By the way, when there are more than one leader AUV, the position estimation of the follower AUV is calculated by using different observation, and the average of multiple position estimations is taken as the final position estimation.

TABLE 1. Pseudo code of the FGMC algorithm.

Algorithm FGMC

Input: d_k, x_k^m, y_k^m, x_{k-1}, y_{k-1}, v_k and θ_k
Output: x_k and y_k

$x_k^- = x_{k-1} + v_k \cos\theta_k \Delta t$
$y_k^- = y_{k-1} + v_k \sin\theta_k \Delta t$
If the observation information is received
  $\Delta x_k^- = x_k^- - x_k^m$
  $\Delta y_k^- = y_k^- - y_k^m$
  $\tilde{d}_k = d_k - \sqrt{(\Delta x_k^-)^2 + (\Delta y_k^-)^2}$
  $\Delta x_k = \Delta x_k^- + e^{-\frac{\tilde{d}_k^2}{2\sigma^2}} \cdot \frac{\tilde{d}_k \Delta x_k^-}{\sqrt{(\Delta x_k^-)^2 + (\Delta y_k^-)^2}}$
  $\Delta y_k = \Delta y_k^- + e^{-\frac{\tilde{d}_k^2}{2\sigma^2}} \cdot \frac{\tilde{d}_k \Delta y_k^-}{\sqrt{(\Delta x_k^-)^2 + (\Delta y_k^-)^2}}$
  $x_k = x_k^- + e^{-\frac{\left(x_k^m + \Delta x_k - x_k^-\right)^2}{2\sigma^2}} \left(x_k^m + \Delta x_k - x_k^-\right)$
  $y_k = y_k^- + e^{-\frac{\left(y_k^m + \Delta y_k - y_k^-\right)^2}{2\sigma^2}} \left(y_k^m + \Delta y_k - y_k^-\right)$
If no observation information is received
  $x_k = x_k^-$
  $y_k = y_k^-$
return x_k and y_k

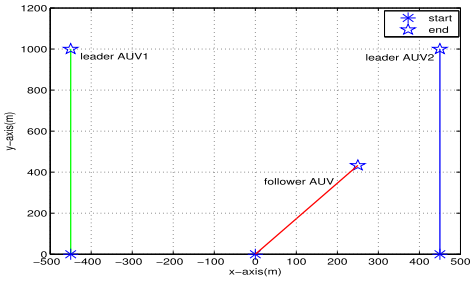

FIGURE 5. Actual AUV trajectory of simulation experiment.

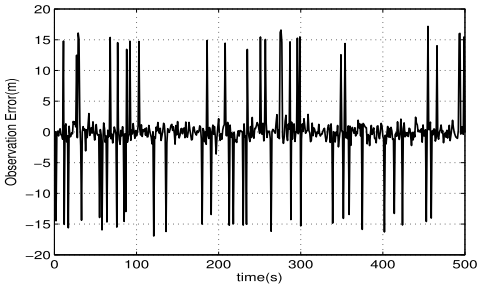

FIGURE 6. Observation error in simulation experiment.

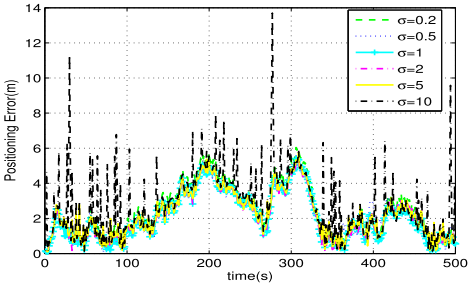

FIGURE 7. Estimated positioning error from different σ.

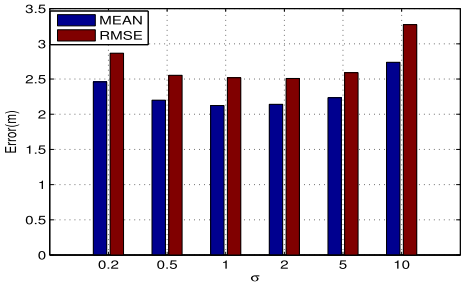

FIGURE 8. Mean and RMSE of estimated positioning error from different σ.

IV. SIMULATION

In this section, we use the simulation experiment of cooperative navigation to verify the effectiveness of the FGMC algorithm proposed in this paper. The RMSE of position is used as performance index. As shown in Fig.5, the two leader AUVs are located on both sides of the follower AUV and sail along the y-axis. The initial positions of the two leader AUV s are $(-450, 0)$ and $(450, 0)$ respectively, and their velocities are 2 m/s. The initial position of follower AUV is (0,0), its heading is 60 degrees, and its velocity is 1 m/s. The sampling interval in the simulation test is 1 s.

In order to facilitate the analysis, the proposed method is compared with EKF, UKF and IFGS algorithms in simulation experiments. In order to simulate the actual observation error, the thick-tailed non-Gaussian measurement noise as shown in Fig.6 is added to the simulation experiment. The simulation time is 500s. The kernel bandwidth of FGMC algorithm determines the credibility of the observation. It should be noted that we cannot choose too small kernel bandwidth because a small bandwidth will make the algorithm close to the DR method. We compared the positioning errors of different σ in the simulation, as shown in Fig.7 and Fig.8. Fig.7 is a positioning error curve figure for selecting different σ. Fig.8 is the mean and RMSE of positioning error with different σ.

We can see from the Fig.8 that the RMSE of positioning error is the smallest when the σ is 2, and the RMSE is 2.507m. The larger the kernel bandwidth of the FGMC algorithm is, the higher the reliability of the observation. So when σ is 5 or 10, the positioning error is greatly affected by the outliers. Thus, we choose 2 as the kernel bandwidth in our proposed algorithm.

Next, the performance of different algorithms are compared. The error of follower AUV from the traditional EKF algorithm [34], the UKF algorithm [35], AREKF algorithm [24], IFGS algorithm [26] and proposed FGMC algorithm are compared under different simulation conditions. By the way, the Intel Core i5-6200U computer was used to simulate experiments, and the time to run the entire simulation of different algorithms is shown in Table 2. And the running time of three simulation of FGMC algorithm is

TABLE 2. Running time of each algorithm.

Algorithm	Simulation 1	Simulation 2	Simulation 3
EKF	0.0347s	0.0353s	0.0345s
UKF	0.0901s	0.0840s	0.0846s
AREKF	0.0603s	0.0505s	0.0529s
IFGS	0.0308s	0.0296s	0.0340s
FGMC	0.0274s	0.0276s	0.0269s

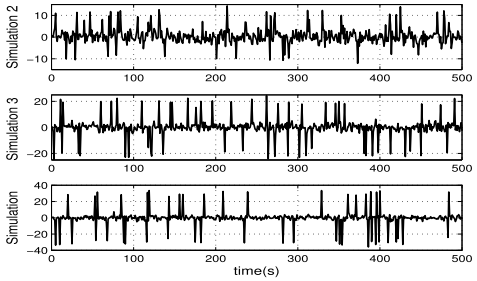

FIGURE 9. Observation error in simulation 2, simulation 3 and simulation 4.

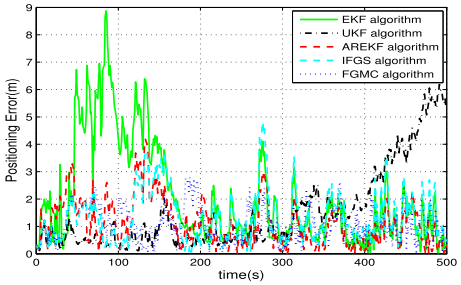

FIGURE 10. Estimated positioning error from different filters in simulation 2.

0.0274s, 0.0276s and 0.0269s, respectively. So we can easily find that the computational complexity of FGMC algorithm is the smallest among these algorithms.

Three simulations are set up to analyze the performance of the algorithm when dealing with outliers of different sizes. In simulation 2, 3 and 4, the outliers of 10m, 20m and 30m are added respectively. Observations of Three simulations are shown in Fig.9. The positioning errors of different algorithms in simulation 2 are shown in Fig.10 and Fig.11. The positioning errors of different algorithms in simulation 3 are shown in Fig.12 and Fig.13. And the positioning errors of different algorithms in simulation 4 are shown in Fig.14 and Fig.15.

In these three simulations, the RMSE of positioning error of FGMC algorithm is 1.2m, 1.2m and 1.3m respectively. It can be seen from Fig.11, Fig.13 and Fig.15 that the proposed FGMC algorithm has the best positioning accuracy in five different algorithm. And this shows that the FGMC algorithm can deal with outliers of different sizes.

V. REAL TESTS AND RESULTS

According to the previous description, we can use boat to replace AUV to verify the algorithm. So in this section, we use

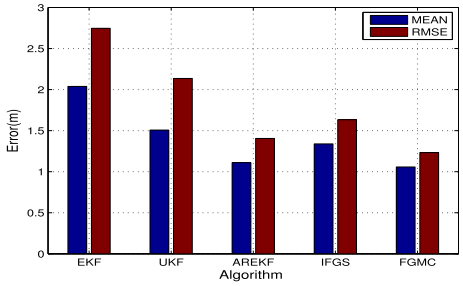

FIGURE 11. Error of each algorithm in simulation in simulation 2.

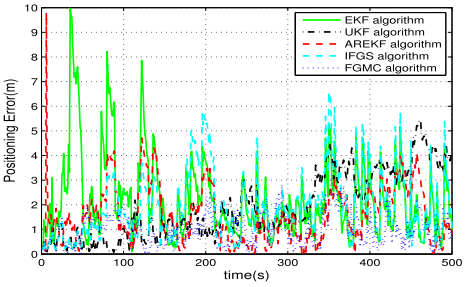

FIGURE 12. Estimated positioning error from different filters in simulation 3.

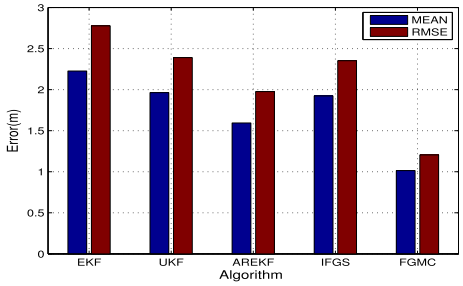

FIGURE 13. Error of each algorithm in simulation in simulation 3.

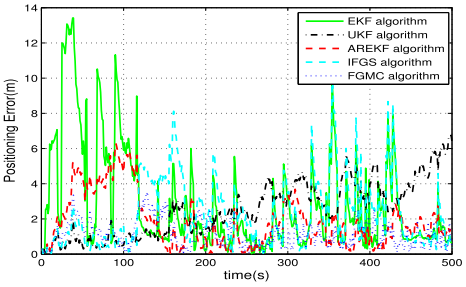

FIGURE 14. Estimated positioning error from different filters in simulation 4.

the data collected by boats in the actual waters to analyze the performance of the proposed FGMC algorithm. In the actual test, we use three boats to test, including two leader boat and one follower boat. And the test time is 3000s.

Both leader boats are equipped with high-precision GPS to obtain accurate position information of the leader boat. The follower boat is equipped with DVL and magnetic compass to obtain speed and course. At the same time, follower boat is

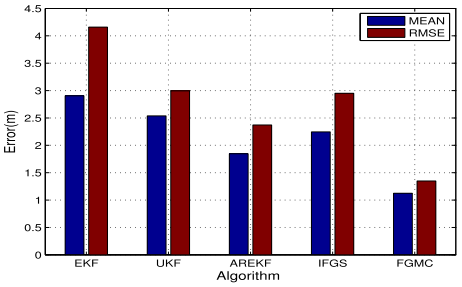

FIGURE 15. Error of each algorithm in simulation in simulation 4.

TABLE 3. Sensors' performance.

Sensor	Performance
GPS	positioning accuracy 2.5m , velocity accuracy 0.1m/s
Compass	Heading accuracy 3°
DVL	velocity accuracy 0.1%
S2CR 7/17	Bit error rate 10^{-10}

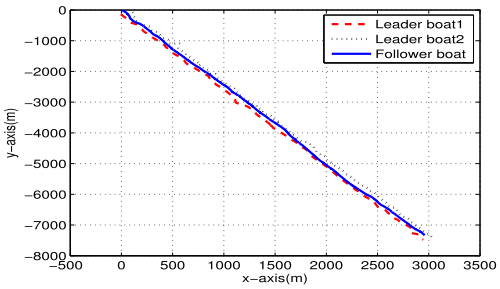

FIGURE 16. Paths taken by the leader and follower boat in test.

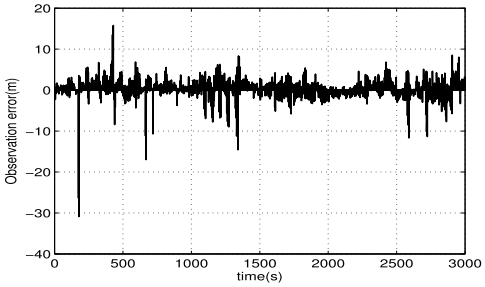

FIGURE 17. Observation error of follower boat in test.

equipped with GPS/PHINS integrated navigation system to provide reference for the results of cooperative positioning. The two leader boats alternately send accurate position and measurement information to follower boat at 5 s interval. Each boat is equipped with an underwater acoustic modem (S2CR 7/17) to build an underwater acoustic communication network. The performance of some sensors in the test is shown in Table 3.

In the experiment, the different trajectories of the three boats are shown in Fig.16. And the error of the observation is shown in Fig.17 and Fig.18. It is found that the standard deviation of the observation error in the experiment is 2.06m. But there are often large outliers.

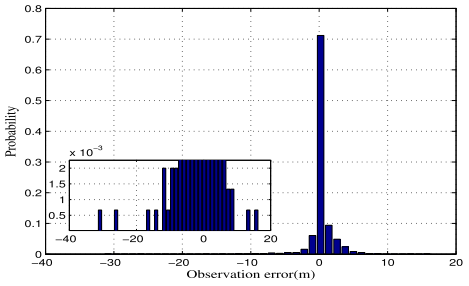

FIGURE 18. The probability distribution of observation error.

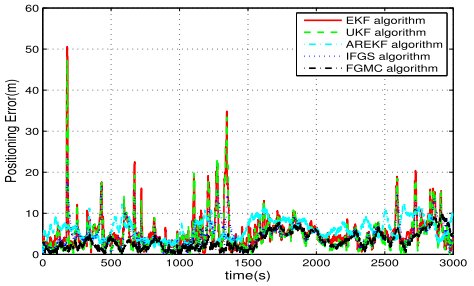

FIGURE 19. Estimated positioning error of follower boat in test.

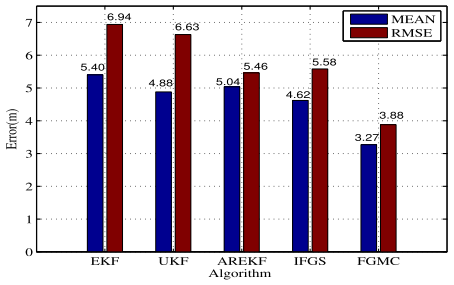

FIGURE 20. Error of each algorithm in test.

The positioning error results of the EKF, UKF, AREKF, IFGS and the proposed FGMC algorithms are shown in Fig.19. In order to compare the results of each algorithm clearly, the mean and RMSE are calculated in Fig.20. From Fig.19 and Fig.20, it is easy to find that the mean and RMSE of the positioning error of the EKF algorithm is the largest among these algorithms. And the mean of EKF algorithm is 5.4 m while the RMSE of EKF algorithm is 6.94 m. Conversely, the FGMC algorithm has the least positioning error, and its mean is 3.24 m while its RMSE is 3.88 m. The experimental results show that the performance of the FGMC algorithm is better than the other 4 algorithms.

VI. CONCLUSION

In this research, a novel FGMC algorithm of cooperative AUV positioning is proposed to reduce positioning error caused by outliers in observations. Through using the proposed FGMC algorithm, the position error of the AUV has been effectively corrected. Specifically, compared with the EKF, UKF, AREKF and IFGS algorithm, the error of the

estimated position (RMSE) derived from the IFGS method reduced by 44.09%, 41.48%, 28.94% and 30.47% in test. The simulation and the real water test results show that the FGMC algorithm achieves higher positioning accuracy, which is expected to provide theoretical research for AUV path planning and multi-AUV CPS.

ACKNOWLEDGMENT

The authors would like to thank the timely help given by Jingchun Li in translation.

REFERENCES

[1] L. Zhang, T. Wang, F. Zhang, and D. Xu, "Cooperative localization for multi-AUVs based on GM-PHD filters and information entropy theory," *Sensors*, vol. 17, no. 10, p. 2286, 2017.
[2] L. Paull, S. Saeedi, M. Seto, and H. Li, "AUV navigation and localization: A review," *IEEE J. Ocean. Eng.*, vol. 39, no. 1, pp. 131–149, Jan. 2014.
[3] L. Stutters, H. Liu, C. Tiltman, and D. J. Brown, "Navigation technologies for autonomous underwater vehicles," *IEEE Trans. Syst., Man, Cybern. C, Appl. Rev.*, vol. 38, no. 4, pp. 581–589, Jul. 2008.
[4] F. Qin, L. Chang, S. Jiang, and F. Zha, "A sequential multiplicative extended Kalman filter for attitude estimation using vector observations," *Sensors*, vol. 18, no. 5, p. 1414, 2018.
[5] C. Yu, H. Lan, F. Gu, F. Yu, and N. El-Sheimy, "A map/INS/Wi-Fi integrated system for indoor location-based service applications," *Sensors*, vol. 17, no. 6, p. 1272, 2017.
[6] C. Yu, N. El-Sheimy, H. Lan, and Z. Liu, "Map-based indoor pedestrian navigation using an auxiliary particle filter," *Micromachines*, vol. 8, no. 7, p. 225, 2017.
[7] Y. Zhang, F. Yu, Y. Wang, and K. Wang, "A robust SINS/VO integrated navigation algorithm based on RHCKF for unmanned ground vehicles," *IEEE Access*, vol. 6, pp. 56828–56838, 2018.
[8] H. Huang, X. Chen, B. Zhang, and J. Wang, "High accuracy navigation information estimation for inertial system using the multi-model EKF fusing adams explicit formula applied to underwater gliders," *ISA Trans.*, vol. 66, pp. 414–424, Jan. 2017.
[9] Q. Sun, Y. Tian, and M. Diao, "Cooperative localization algorithm based on hybrid topology architecture for multiple mobile robot system," *IEEE Internet Things J.*, vol. 5, no. 6, pp. 4753–4763, Dec. 2018.
[10] C. Sun, Y. Zhang, G. Wang, and W. Gao, "A new variational Bayesian adaptive extended Kalman filter for cooperative navigation," *Sensors*, vol. 18, no. 8, p. 2538, 2018.
[11] Y. Liu, "Research on cooperative localization algorithm for multiple autonomous underwater vehicles," Ph.D. dissertation, College Automat., Harbin Eng. Univ., Harbin, China, 2015.
[12] L. Chang, F. Zha, and F. Qin, "Indirect Kalman filtering based attitude estimation for low-cost attitude and heading reference systems," *IEEE/ASME Trans. Mechatronics*, vol. 22, no. 4, pp. 1850–1858, Aug. 2017.
[13] L. Zhang, W. Gao, Q. Li, R. Li, Z. Yao, and S. Lu, "A novel monitoring navigation method for cold atom interference gyroscope," *Sensors*, vol. 19, no. 2, p. 222, Jan. 2019.
[14] J. R. Millar, D. D. Hodson, G. B. Lamont, and G. L. Peterson, "Multi-objective optimization of dead-reckoning error thresholds for virtual environments," in *Proc. Int. Conf. Collaboration Technol. Syst.*, 2014, pp. 562–569.
[15] B. Allotta, R. Costanzi, E. Meli, L. Pugi, A. Ridolfi, and G. Vettori, "Cooperative localization of a team of AUVs by a tetrahedral configuration," *Robot. Auto. Syst.*, vol. 62, no. 8, pp. 1228–1237, Aug. 2014.
[16] F. Sun, H. Lan, C. Yu, El-Sheimy, Naser, G. Zhou, T. Cao, and H. Liu, "A robust self-alignment method for ship's strapdown INS under mooring conditions," *Sensors*, vol. 13, no. 7, pp. 8103–8139, 2013.
[17] Y. Zhang, F. Yu, W. Gao, and Y. Wang, "An improved strapdown inertial navigation system initial alignment algorithm for unmanned vehicles," *Sensors*, vol. 18, no. 10, p. 3297, Oct. 2018.
[18] M. F. Fallon, G. Papadopoulos, J. J. Leonard, and N. M. Patrikalakis, "Cooperative AUV navigation using a single maneuvering surface craft," *Int. J. Robot. Res.*, vol. 29, no. 12, pp. 1461–1474, Oct. 2010.
[19] G. Jia, H. Bo, and H. Duan, "Intelligent assistance positioning methodology based on modified iSAM for AUV using low-cost sensors," *Ocean Eng.*, vol. 152, pp. 36–46, Mar. 2018.
[20] S. J. Julier and J. K. Uhlmann, "New extension of the Kalman filter to nonlinear systems," *Proc. SPIE*, vol. 3068, pp. 182–194, Jul. 1997.
[21] M. Nørgaard, N. K. Poulsen, and O. Ravn, "New developments in state estimation for nonlinear systems," *Automatica*, vol. 36, no. 11, pp. 1627–1638, 2000.
[22] C. D. Karlgaard and H. Schaub, "Huber-based divided difference filtering," *J. Guid. Control Dyn.*, vol. 30, no. 3, pp. 885–891, May 2007.
[23] W. Gao, Y. Liu, and B. Xu, "Robust huber-based iterated divided difference filtering with application to cooperative localization of autonomous underwater vehicles," *Sensors*, vol. 14, no. 12, pp. 24523–24542, 2014.
[24] K. Xiong, H. Zhang, and L. Liu, "Adaptive robust extended Kalman filter for nonlinear stochastic systems," *IET Control Theory Appl.*, vol. 2, no. 3, pp. 239–250, Mar. 2008.
[25] L. Chang, B. Hu, G. Chang, and A. Li, "Huber-based novel robust unscented Kalman filter," *IET Sci. Meas. Technol.*, vol. 6, no. 6, pp. 502–509, Nov. 2012.
[26] S. Fan, Y. Zhang, C. Yu, M. Zhu, and F. Yu, "An advanced cooperative positioning algorithm based on improved factor graph and sum-product theory for multiple AUVs," *IEEE Access*, vol. 7, pp. 67006–67017, 2019.
[27] F. R. Kschischang, B. J. Frey, and H.-A. Loeliger, "Factor graphs and the sum-product algorithm," *IEEE Trans. Inf. Theory*, vol. 47, no. 2, pp. 498–519, Feb. 2001.
[28] B. Chen and J. C. Principe, "Maximum correntropy estimation is a smoothed MAP estimation," *IEEE Signal Process. Lett.*, vol. 19, no. 8, pp. 491–494, Aug. 2012.
[29] W. Liu, P. P. Pokharel, and J. C. Principe, "Correntropy: Properties and applications in non-Gaussian signal processing," *IEEE Trans. Signal Process.*, vol. 55, no. 11, pp. 5286–5298, Nov. 2007.
[30] S. Zhao, B. Chen, and J. C. Príncipe, "Kernel adaptive filtering with maximum correntropy criterion," in *Proc. Int. Joint Conf. Neural Netw.*, 2011, pp. 2012–2017.
[31] A. Singh and J. C. Príncipe, "A loss function for classification based on a robust similarity metric," in *Proc. Int. Joint Conf. Neural Netw.*, 2010, pp. 1–6.
[32] L. Xi, B. Chen, H. Zhao, J. Qin, and J. Cao, "Maximum correntropy Kalman filter with state constraints," *IEEE Access*, vol. 5, pp. 25846–25853, 2017.
[33] B. Chen, X. Liu, H. Zhao, and J. C. Principe, "Maximum correntropy Kalman filter," *Automatica*, vol. 76, pp. 70–77, Feb. 2017.
[34] S. S. Kia, S. Rounds, and S. Martínez, "Cooperative localization under message dropouts via a partially decentralized EKF scheme," in *Proc. IEEE Int. Conf. Robot. Autom.*, May 2015, pp. 5977–5982.
[35] S. Xingxi, H. Bo, W. Tiesheng, and Z. Chunxia, "Cooperative multi-robot localization based on distributed UKF," in *Proc. IEEE Int. Conf. Comput. Sci. Inf. Technol.*, Jul. 2010, pp. 590–593.

SHIWEI FAN was born in 1993. He received the B.S. degree from the Department of Automation, Harbin Engineering University, Harbin, China, in 2015. He is currently pursuing the Ph.D. degree in instruments science and technology with the Harbin Institute of Technology. His current research interests include inertial navigation systems and cooperative navigation systems.

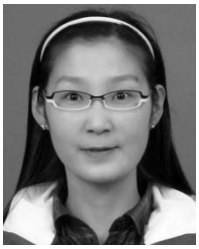

YA ZHANG received the B.Eng. and Ph.D. degrees from Harbin Engineering University, Harbin, Heilongjiang, China, in 2010 and 2015, respectively. She holds a postdoctoral position at the School of Instrumentation Science and Engineering, Harbin Institute of Technology, Harbin. Her current research interests include vision-based mobile robot navigation systems and multisensor information fusion.

QIANG HAO was born in 1992. He received the B.S. degree from the Department of Automation, Harbin Engineering University, Harbin, China, in 2015. He is currently pursuing the Ph.D. degree in instruments science and technology with the Harbin Institute of Technology. His current research interests include inertial navigation systems and indoor positioning systems.

PAN JIANG was born in 1993. He received the B.S. degree from the Department of Automation, Harbin Engineering University, Harbin, China, in 2015. He is currently pursuing the Ph.D. degree in instruments science and technology with the Harbin Institute of Technology. His current research interest includes inertial navigation systems.

CHUNYANG YU received the Ph.D. degrees in positioning, navigation and wireless location from the University of Calgary, and measuring and testing technologies and precision instruments and machinery from the Harbin Engineering University. She is currently a Postdoctoral Fellow with the Mobile Multi-Sensor Systems (MMSS) research group, University of Calgary, Calgary, Canada.

FEI YU received the B.S. degree from the Dalian University of Technology, in 1997, and the M.Eng. and Ph.D. degrees from Harbin Engineering University, Harbin, China, in 2003 and 2005, respectively. He is currently a Professor with the School of Instrumentation Science and Engineering, Harbin Institute of Technology. His current research interest includes inertial navigation systems.